Responses of HIII, THOR and SAFER-HBM occupant models in rearward-facing seat configuration for high severity frontal impact

Anurag Soni, Stefan Schilling, Jan Faust and Burkhard Eickhoff

Abstract Rearward-facing seat was proposed as one of the potential seating configurations for highly automated vehicles. The objective of this paper was to understand the responses of existing Anthropometric Test Devices (ATDs) for the rearward-facing seat configuration in full-frontal impact. Therefore, a finite element simulation model of a generic rearward facing seat validated against the test results was utilized. The 50th percentile male versions of the THOR, the H350 and the SAFER-Human Body Model (SAFER-HBM) were positioned and simulations for rear impact were performed according to FMVSS208 at 56 km/h. Effects of seatback rotational stiffness were also investigated. Based on the results, the THOR response was found closer to the SAFER-HBM in several aspects than H350. While both ATDs matched kinematics and accelerations of the SAFER HBM reasonably well, only THOR and SAFER HBM could capture inertially induced deformation in the chest.

Keywords Autonomous Driving, Rearward Facing Seat, Vehicle Restraints, H350, THOR, SAFER-HBM, Finite Element Models

I. INTRODUCTION

The development of automated driving would allow new seating configurations in future automobiles [1, 2]. For example, front seats could be swiveled to create a living room seating situation for better interaction with the 2nd row passengers [2]. This implies that the front row passengers would then be sitting in a rearward-facing seat configuration. Even when fully-automated vehicles replace the conventional vehicles, the risk of an accident cannot be avoided, though accidents of the future will differ from those of today [3, 4, 5]. Therefore, occupant protection must not be compromised and should be independent of seating orientation [6]. This means that in a frontal crash the front row passenger seated in rearward-facing configuration will be loaded in the opposite direction of motion compare to same situation today with traditional seating. The existing restraint systems have been designed, optimized and thus are better suited for the forward-facing seat configuration. An optimization of a restraint system for rearward facing seat configuration including seat belt and pre-tensioners has not been done so far however the effect of pre-tensioners has shown benefit in reducing occupant displacement [7]. Recently, it was shown that given adequate seat stiffness and sufficient space between backrest and hard structure, a combination of seat energy management together with active head and backrest could deliver good protection [8].

Current Anthropometric Test Devices (ATDs), except the BioRid, are developed and validated for frontal impact or side impact and are therefore not optimal for evaluating occupant restraint functions in a rearward impact. Additionally, the BioRID is only used for low speed rear impacts. At the current state and given the prevalence of physical testing in the evaluation of occupant safety, it is important to study the strengths and limitations of the existing ATDs for their use in rear-facing high-speed impacts. However, there are limited biomechanical targets as of now to rate their responses.

Only recently, in an on-going project, first series of high-speed rear impact tests were performed with Post Mortem Human Subjects (PMHS) for the rearward-facing seat configuration at Ohio State University [9]. Although an adjustable setup was built to measure seat reaction forces, the seatback was supported with a rigid support. Tests were conducted for two sled pulses (delta-V of 24 km/h and 56 km/h) and two seat back reclined angles (25 degrees and 45 degrees). Though minor cervical spine injuries were found in all the cadavers, there were seatback structure related fractures in scapula and in several ribs (both in anterior and posterior side).

Dr A. Soni (e-mail: anurag.soni@autoliv.com, tel: +49-41217975620), S. Schilling, J. Faust and Dr B. Eickhoff work at Autoliv North Germany

From the accident data analysis perspective, few car models are equipped with rearward facing seats and almost no analysis focusing on adult car occupants on rearward facing seats has been published. An analysis of the German In-Depth Accident Study (GIDAS) identified only five cases with rearward facing adult occupants in passenger cars. Only one occupant on a rearward facing seat was moderately injured, but in all collisions the delta-V of the impacted vehicle was below 25 km/h [6]. In another study [10], an investigation was reported on 1,000 fatalities occurred in 2015 in the US in rear struck passenger cars and light trucks. Most fatal crashes appeared to involve compartmental collapse, which was present in 4.4% of all rear impact crashes. The study suggested that besides direct head impact to rigid interior vehicle structures, thoracic loading from the seat as the source of injury. Furthermore, rib fractures, serious upper and lower extremity fractures and cervical-spine fractures were reported. These finding match well with injuries found in Ohio State University PMHS testing [9].

Normally sled testing in the rearward occupant loading direction was mainly to determine neck injury risk in low speed rear impacts. Some studies were performed to determine injury risk in rear impacts with a delta-V of up to 40 km/h [11, 12]. It was reported that dummy response was strongly related to seat design especially its stiffness in rearward rotation. In addition to studies that were mainly based on tests, simulation studies using human FE model - Total Human Model for Safety (THUMS) on rearward facing seats in full frontal impact conditions were also published. Occupant kinematics was described for three crash speeds (i.e. 56 km/h, 40 km/h and 30 km/h) on both rearward and forward facing along with intermediate orientations [13]. For the rear facing seat, it was reported that the occupant head moved upwards along the seatback and shown that the neck loading was the highest. Injury risk was compared in different loading directions [14] and it was concluded that the rearward facing seating position showed the lowest injury risk. Lately, biofidelity of the Global Human Body Models Consortium (GHBMC) average male occupant HBM was evaluated against PMHS rear-impact tests at two severities (17 km/h and 24 km/h) [15]. The HBMs exhibited gross kinematics observed in the PMHS tests generally well however validation was limited to only low severity range. The objective of this study is to compare existing ATD currently used for evaluation of frontal impacts, i.e. H350 and THOR 50% with the SAFER-HBM in terms of kinematic, acceleration, forces and moments to understand similarities and differences when restraint by a seat back and a state of the art 3-point belt without pretensioner. The comparison is to be made in a rearward-facing seat configuration and with a typical full-frontal impact pulse according to FMVSS208 at 56 km/h. It is important to mention that none of the chosen occupant models in this study are validated for rear facing high speed impact and therefore objective here is not to evaluate their biofidelity but only to compare their responses.

II. METHODS

Generic Seat and Physical Sled Test

A generic seat (Figure 1) having controlled rearward rotational stiffness of backrest including energy dissipation was developed and three test series were conducted with H350 dummy [16]. The seat consists of a stiff seat-pan, a backrest and a headrest. The seat-pan was rigidly fixed to the sled floor. The headrest was rigidly fixed to the backrest and the backrest was connected to the sled floor via ball bearings at both the sides. The ball bearings thus allowed the backrest to freely rotate relative to the sled. The required stiffness to the ball bearing joint was achieved by connecting the backrest to a steel frame also mounted on the sled with two layers of webbing each side of the backrest. The rearward displacement and the energy dissipation during the crash therefore could be controlled by deformation in the webbing layers. Each of the four layers of webbing has the standard stiffness i.e. 10 kN force at 12% elongation. It was decided to set the initial dummy torso angle at 25 degrees from the vertical and this could be achieved with 1200 mm long webbing in the front.

A H350 male dummy was seated on the generic seat and a series of repeatability tests with the generic test environment were performed [16]. Among different restraint combinations, a set of identical tests with standard 3-point belt system without belt pretensioner was performed with the aim to generate enough test data for performing model validation.

Computational Modeling

A FE simulation model of the test set-up (i.e. H350 model seated on generic seat with standard 3-point belt system without belt pretensioner) was created in LS-Dyna solver environment and validated against the test results. It was shown that simulation results match closely to the test results [17]. A summary of validation results is given in the appendix A1 and more details could be found in [17]. The validated seat model was

utilized in the current investigation.

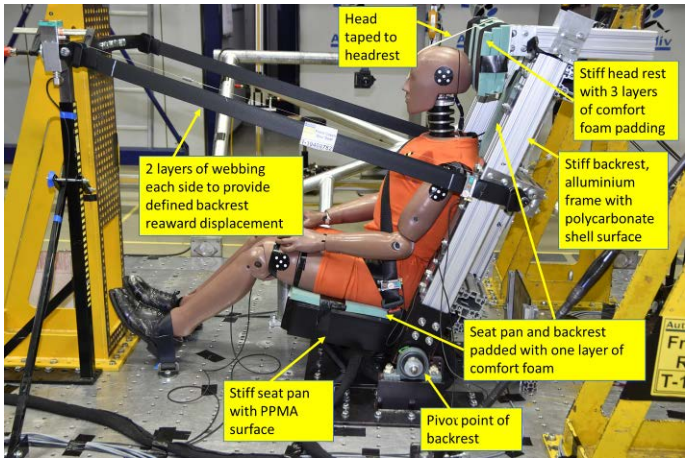

Fig. 1. Test set-up showing H350 seated in the generic rearward facing seat environment

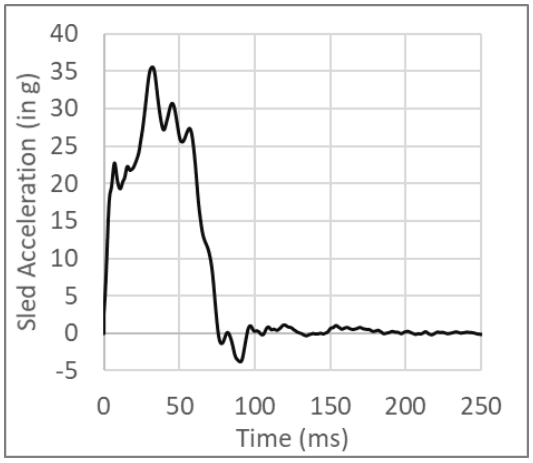

Fig. 2. The crash pulse derived from repeatability tests also utilized in simulations

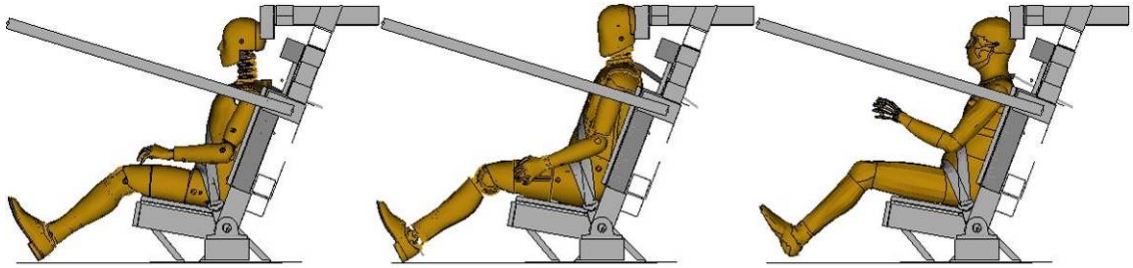

Fig. 3. Simulation set-up: H350 (in the left), THOR (in the middle) and SAFER-HBM (in the right) seated in the generic rearward facing seat environment

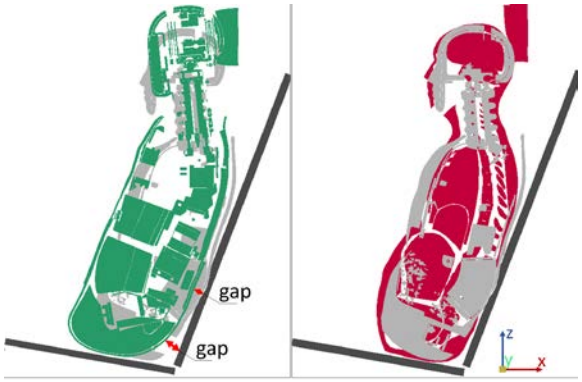

Fig. 4. Overlaid centroidal cut section of H350 (in grey) and THOR (in green, in left) and SAFER-HBM (in red, in right) at initial stage

The 50th percentile male versions of the THOR, H350 and SAFER-HBM models were positioned in the seat model. Figure 3 shows the simulation set-up after positioning all the three occupant models on the generic seat. While the H350 model was positioned using the H-point and other marker positions available from the tests, the THOR and the SAFER-HBM were positioned taking H350 as a target. The SAFER-HBM could be positioned close to the H350 (see Figure 4), however it was under achieved with THOR positioning. The H350 has a hump in the back due to lumbar spine whereas the THOR has relatively straighter back and a curvature with lower radius in the buttock area. Due to these differences, a gap was left between the THOR's back to seat backrest (marked in Figure 4) while reasonably matching the torso and the neck angle. Finally, for the given THOR position, the H-point was 25 mm forward in x-direction and 46 mm higher in z-direction as compared to that of H350. After positioning each occupant model, seat squashing was performed, and seatbelt was routed in PRIMER^{TM}. The effect of backrest rotational stiffness was also investigated. Therefore, in addition to the reference rotating backrest having stiffness equivalent to four layers of front webbing, one variation of infinite stiffness (named as fixed backrest) was also simulated. In the model, the ball bearing which connects the backrest to the sled floor in the physical seat was effectively modeled using one six degree of freedom beam element each side in the

simulation model. For the reference rotating backrest, the rotation of the beam about y-axis was defined with null stiffness whereas other degree of freedoms was set to very high stiffness. To simulate the fixed backrest, beam element was assigned a sufficiently high rotation stiffness about the y-axis that it behaved as if it was locked. Thereby, effect of front webbing was nullified. In total, six simulations (2 backrest variation and 3 occupant models) for rear facing impact were performed with the pulse intensity representing a full-frontal impact according to FMVSS208 at 56 km/h. The average crash pulse derived from the repeatability tests was used in the current simulations (Figure 2) which led to a delta-V of about 60 km/h.

To achieve a qualified comparison, responses of the occupant models were compared in terms of overall kinematics, force on backrest, trajectories (head, chest and pelvis), acceleration (chest and pelvis), chest deflection, forces and moments in the lumbar and cervical spine, and finally deformation in the abdominal organs. For calculating the trajectories, predefined markers in the dummy outputs for head center of gravity (CoG), T4 (for chest), and pelvis CoG were utilized. Signals from accelerometer nodes defined at T4 and pelvis were filtered with CFC1000 and utilized for chest and pelvis accelerations, respectively. Chest deflection was being calculated differently in each occupant model. In SAFER-HBM, six discreet beams (shown in Figure B1 in appendix B1) were implemented for easy chest deflection measurement [18]. The maximum deflection out of the six beams was selected as chest deflection in SAFER-HBM. In THOR, four IRTRACCs are implemented and the maximum of the four was selected as THOR chest deflection. In H350, output from chest deflection measurement beam was used. In the SAFER-HBM, database sections are defined in cervical spine at each vertebra i.e. from C2 to C7 levels and in each lumbar vertebra from L1 to L5. The section forces and moments for SAFER-HBM at C2 level was named as upper neck whereas C7 level was named as lower neck. Similarly, L1 was named as upper lumbar and L5 was named as lower lumbar. For both THOR and H350 models, the load cells at upper and lower neck were utilized to calculate upper neck and lower neck forces and moments, respectively. For the H350 model, loadcells defined as upper lumbar and lumbar were utilized to calculate force and moment at the upper lumbar and lower lumbar levels, respectively. Whereas, in the THOR model, only one load cell is defined at T12 level which was utilized to calculate upper lumbar force and moment. No lower lumbar values are therefore calculated for the THOR model.

III. RESULTS

Figure 5 show the kinematics of the occupant models at different instances in the simulations for the rotating backrest and the fixed backrest cases. The overall kinematics look similar among all three occupant models for each simulated variation. Irrespective to the seat backrest stiffness, since the direction of motion is opposite to seating direction, the occupant models move into the backrest and thus away from the belt systems. The upper body is pushed against the backrest leading to extension in spinal column, pelvis rotation and eventually sliding upwards on the backrest. The pelvis then leaves contact with the seat-pan and lower legs impact the front of the seat-pan. While the upper body continues to slide upwards, the head is restraint by the headrest. This causes shoulders to move into the gap between the backrest and the headrest, leading to deformation in the neck. At the end of loading phase (around 75 ms), occupant models go into rebound phase. Unlike in conventional forward-seating configuration where seatbelt contributes in restraining the occupant, in rearward-facing seat configuration the seat backrest restrains the occupant models whereas interaction with belts is found effective during rebound. Amongst the three occupant models the THOR slides comparatively higher on the seat backrest such that at 75 ms, the shoulders of the THOR reach close to the headrest and the head goes above the top of the headrest. In contrast, such a displacement is not prominent for both SAFER-HBM and H350.

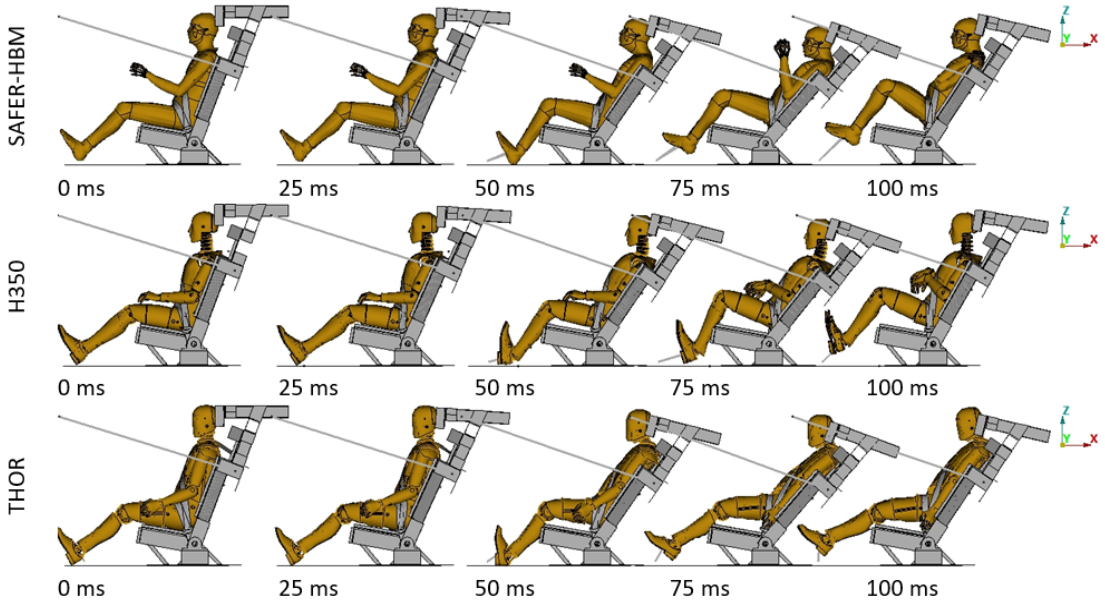

(a) with rotating backrest

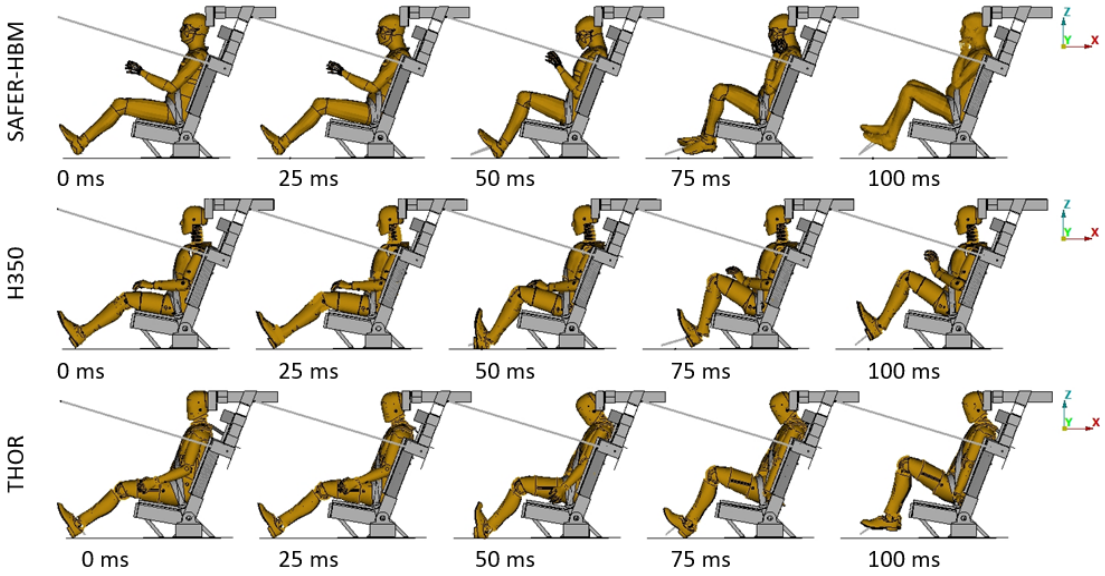

(b) with fixed backrest

Fig. 5. Kinematics of occupant models at different instances with (a) rotating backrest and (b) fixed backrest

Figure 6 compares head, chest and pelvis trajectories in x and z directions relative to sled floor for all the three occupant models and for two variations in the seat backrest rotational stiffness. Table 1 summarizes the peak displacements achieved by the head CoG, the chest (at T4) and the pelvis CoG for both the backrest stiffness cases. It is observed from Figure 6 that the initial positions of the head CoG, chest (T4) and pelvis CoG markers used for calculating the trajectories are different amongst the occupant models due to differences in body dimensions and seating positions. While the differences are within 30 mm in x-direction, except for the pelvis CoG which is the largest (about 100 mm) between THOR and SAFER-HBM, these differences are larger in the z-direction. The THOR's head CoG marker is 70 mm higher than the H350 (which has the lowest head CoG position) whereas, the SAFER-HBM's T4 position is 105 mm above the H350.

While moving rearwards with the rotating backrest, THOR peak displacements are overall closer to SAFER-HBM as compared to H350. The peak head displacements in THOR are within 10 - 15 mm difference in both x and z-direction to that in SAFER-HBM whereas it is at least 35 mm lower in z-direction in H350 than others. Compared to SAFER-HBM, peak chest displacements in both THOR and H350 are substantially lower. The peak is lower by 55 mm in x and 25 mm in z in H350 compared to SAFER-HBM. In contrast to the rotating backrest, with the fixed backrest, all the displacements are substantially lower. Amongst all, the H350 has the lowest displacements at all marker positions. The head and chest trajectories are close between the THOR and the

SAFER-HBM however, pelvis displacement differs between them. While pelvis in SAFER-HBM goes in negative z-direction (-6 mm), it lifts in positive z-direction in THOR (+ 15 mm).

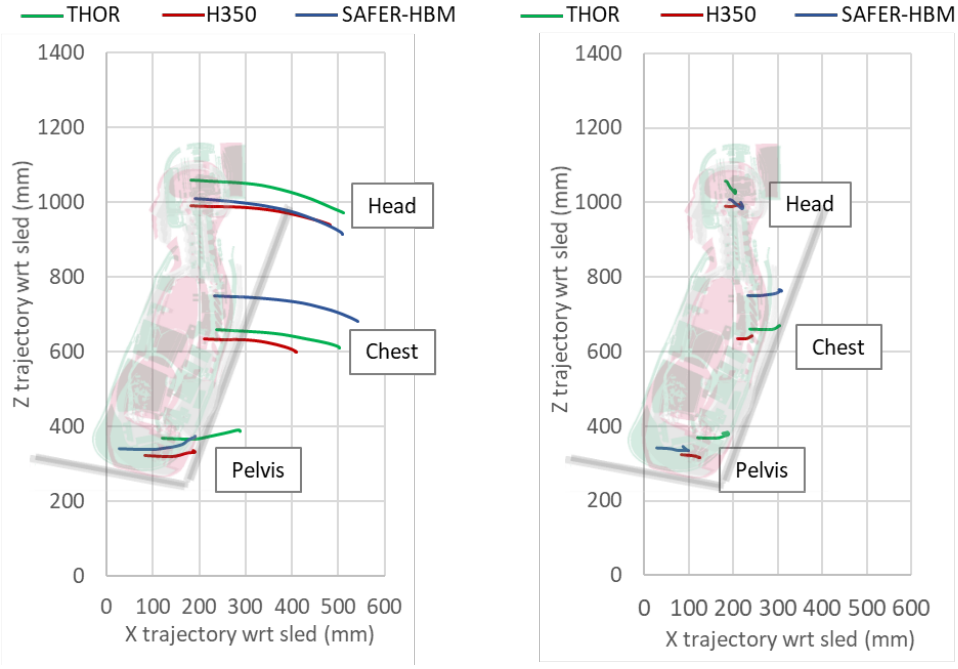

Fig. 6. Comparison of head, chest and pelvis trajectories relative to sled floor among the occupant models for the simulated variations only during loading phase i.e. until 75 ms (rebound is excluded): rotating backrest (in the left) and fixed backrest (in the right)

TABLE I

PEAK DISPLACEMENTS

Peak displacements in Head, Chest and Pelvis: In rotating backrest case (unit in mm)						
	THOR		H350		SAFER-HBM	
	x	z	x	z	x	z
Head	330	-86	300	-51	318	-95
Chest	265	-50	198	-36	310	-70
Pelvis	168	18	108	8	163	33

Peak displacements in Head, Chest and Pelvis: In fixed backrest case (unit in mm)						
	THOR		H350		SAFER-HBM	
	x	z	x	z	x	z
Head	23	-30	32	5	30	-22
Chest	65	11	31	9	75	12
Pelvis	66	15	43	-7	70	-6

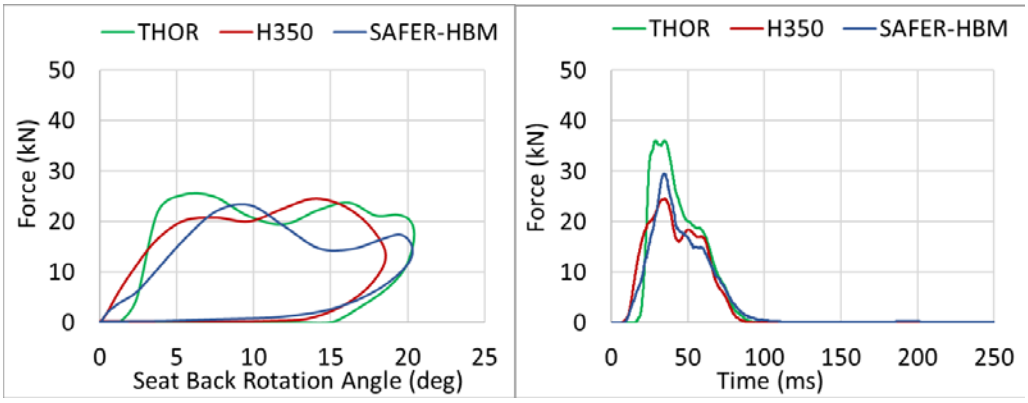

Fig. 7. Comparison of contact force between seat backrest to occupant models as a function of seatback rotation angle for rotating backrest (in the left) and time history for fixed backrest (in the right)

Figure 7 compares the contact force between the backrest and the occupant model for both the backrest stiffness cases. For the rotating backrest, contact force is plotted against the seatback rotation angle whereas contact force time history is plotted for the fixed backrest case. While, peak force values in the rotating backrest

are similar amongst the occupant models (about 25 kN), the maximum rotation in the seatback is lower by about 2.5 degrees with H350 (peak 18.6 degrees) as compared to other occupant models (20.2 degrees with both THOR and SAFER-HBM). Compared to rotating backrest, the peak force values are in general higher in the fixed backrest case and the difference amongst the occupant models is also higher (35 kN in the THOR, 29.5 kN in SAFER-HBM and 25 kN in H350).

Figure 8 and Figure 9 compares chest and pelvis resultant accelerations for all the three occupant models for the two variations in the seat backrest stiffness. Irrespective to backrest stiffness, the THOR has similar peak accelerations in chest and in pelvis to that to SAFER-HBM whereas chest acceleration in H350 (40 g) with the fixed backrest is lower by about 30 g compared to SAFER-HBM (65 g) and THOR (73 g).

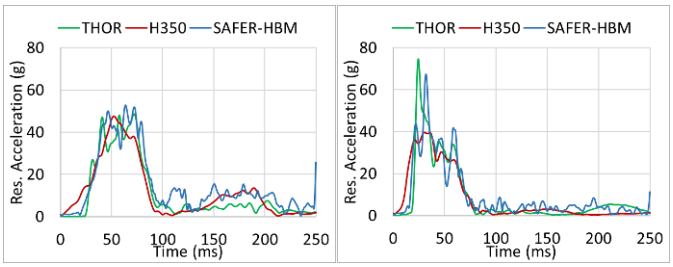

Fig. 8. Comparison of chest acceleration among the occupant models for the simulated variations: rotating backrest (in left), fixed backrest (in right)

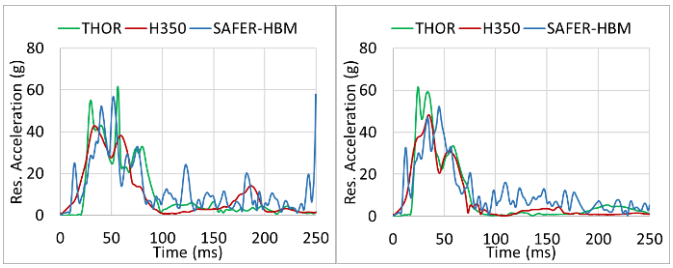

Fig. 9. Comparison of pelvis acceleration among the occupant models for the simulated variations: rotating backrest (in left), fixed backrest (in right)

Figure 10 (a) compares the maximum chest deflection, whereas Figure 10 (b) shows deformation in rib cage in the three occupant models for the two variations in the seat backrest stiffness. For SAFER-HBM, the mid-sternum spring (between sternum center to vertebra at rib-6) gives the maximum chest deflection in both the cases. For THOR, the maximum of all four IRTRACCs is taken for the comparison and in both the cases it is in upper left IRTRACC. For H350, it is the mid sternum spring for chest deflection output. It is shown in Figure 10 (a) that irrespective to the seat backrest rotational stiffness, the maximum chest deflection for the THOR (peak values are 35 mm and 60 mm in rotating and fixed backrest, respectively) is within 10 mm difference to the maximum chest defection calculated for the SAFER-HBM (peak values are 46 mm and 50 mm in rotating and fixed backrest, respectively), whereas, chest deflection in H350 are very low (peak value is less than 5 mm) independent to the backrest stiffness configurations.

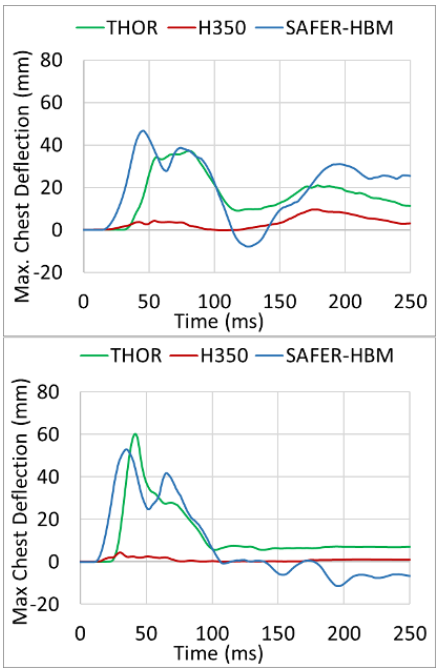

Fig. 10 (a). Comparison of maximum chest deflection for the simulated variations: rotating backrest (above), and fixed backrest (below)

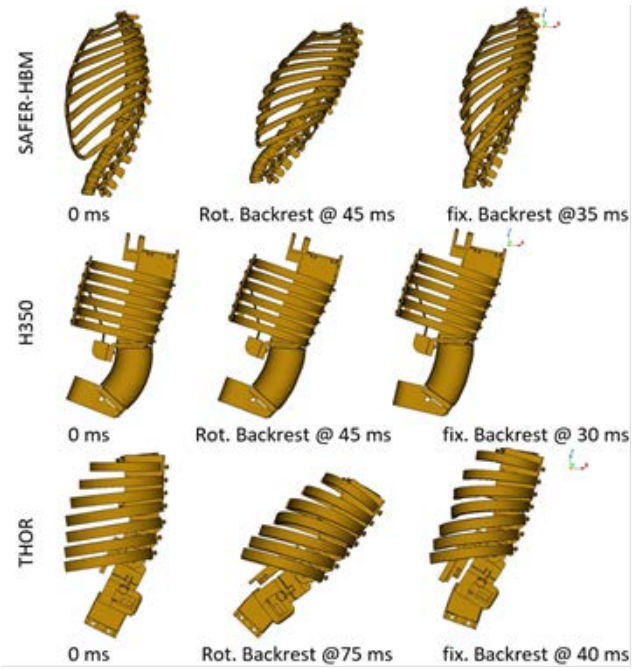

Fig. 10 (b). Deformation in thorax at the time of maximum chest deflection

Figure 11 and Figure 12 compares the tension-compression force and flexion-extension moment time histories in upper and lower lumbar spine among the three occupant models for the two variations in the seat backrest stiffness, respectively. It is shown in Figure 11 that with the rotating backrest, the peak compression forces in the upper lumbar spine are nearly same for the SAFER-HBM and H350 (about 2 kN) whereas it is 2 times higher in THOR (4 kN). However, with the fixed backrest, compression force increases to 3.6 kN in H350 and to 4.5 kN in THOR whereas reduces to 1.2 kN in the SAFER-HBM. Irrespective to the backrest stiffness, the extension moment in H350 and THOR follow similar profile, though with lower peak values in THOR (150 Nm and 175 Nm with rotating and with fixed backrest respectively) compared to H350 (257 Nm and 228 Nm with rotating and with fixed backrest respectively), whereas, it remains below 20 Nm in the SAFER-HBM.

Figure 12 compares the tension-compression force and flexion-extension moment in lower lumbar spine for the simulated variations. For the SAFER-HBM, while the peak compression force reaches 2 kN (with rotating backrest) and 1.2 kN (with fixed backrest), the peak extension moment remains less than 10 Nm in both the cases. In comparison to SAFER-HBM, both compression force and moment are much higher in H350. For H350, the peak compression force reaches above 5 kN and the peak moment goes above 150 Nm in both the backrest cases.

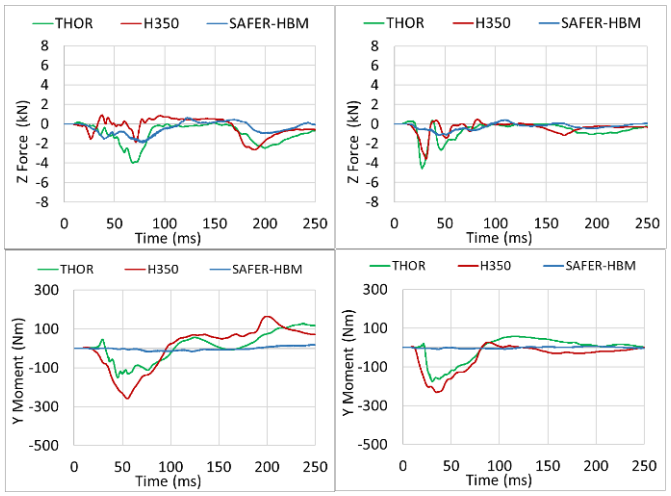

Fig. 11. Comparison of tension-compression force and flexion-extension moment in upper lumbar for the simulated variations: rotating backrest (in the left), fixed backrest (in the right)

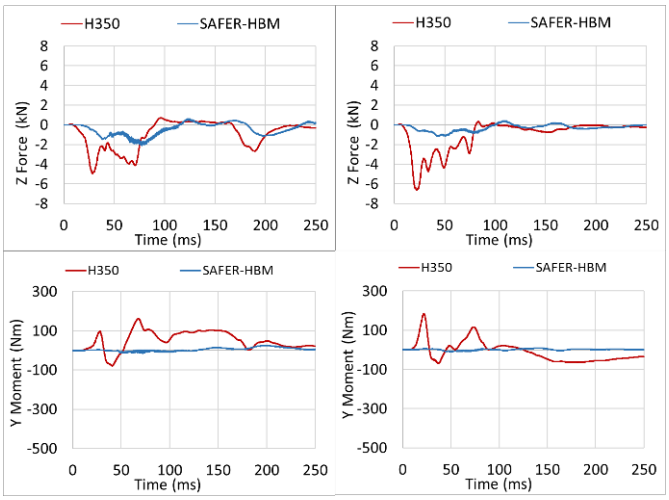

Fig. 12. Comparison of tension-compression force and flexion-extension moment in lower lumbar for the simulated variations: rotating backrest (in the left), fixed backrest (in the right) (Note: No channel is available in the THOR therefore results could not be included)

Figure 13 and Figure 14 compares the tension-compression force and Y-moment in upper and lower cervical spine among the three occupant models for the two variations in the seat backrest stiffness, respectively. It can be seen in Figure 13 that for both the backrest variations the peak values of compression force are close between THOR (1.96 kN and 1.9 kN in rotating and fixed backrest, respectively) and SAFER-HBM (1.6 kN and 1.96 kN in rotating and fixed backrest, respectively) whereas the peak values in the H350 (0.8 kN and 1.3 kN in rotating and fixed backrest, respectively) are about 50% less than that in the THOR. For the rotating backrest, while, the peak flexion-extension moment values are 9 times higher in THOR (- 45 Nm) and 5 times higher in H350 (+ 27 Nm) than in the SAFER-HBM (+5 Nm), the sign is also opposite between THOR and H350. This means while THOR neck is loaded in extension whereas H350 neck exhibit flexion, whereas loading has shifted initially from extension to later in flexion in the SAFER-HBM. These differences have changed with the fixed backrest case, not only the difference in the peak flexion-extension moment values reduced, loading is also in flexion among all three occupant models.

It is observed that for both the backrest cases while compression force response for the lower cervical spine (Figure 14) in the THOR is closer to that in the SAFER-HBM, the THOR flexion moment response is quite different. While for the rotating backrest the peak value in THOR (3.3 kN) is higher by 1 kN than in the SAFER-HBM (2.3 kN), it matches quite closely both in terms of peak values and nature of curve in the fixed backrest

case (peak compression force is 2.3 kN in both THOR and SAFER-HBM). While the difference between the H350 (peak value of 1 kN) to the SAFER-HBM is larger by 1.3 kN in the rotating backrest, the peak in H350 (1.6 kN) reaches close to the SAFER-HBM (2.3 kN) in the fixed backrest case. For the rotating backrest, the peak value of flexion moment is the highest in the THOR (200 Nm) whereas it is only 40 Nm in the SAFER-HBM. In the H350, the peak value reaches to 140 Nm however it occurs during the rebound phase (about 220ms). The highest value in the loading phase (i.e. before 75 ms) reaches 38 Nm which is close to that in SAFER-HBM. With the fixed backrest, the THOR peak reduced to 116 Nm and is close to the H350 (88 Nm), however it remains higher as compared to SAFER-HBM (30 Nm).

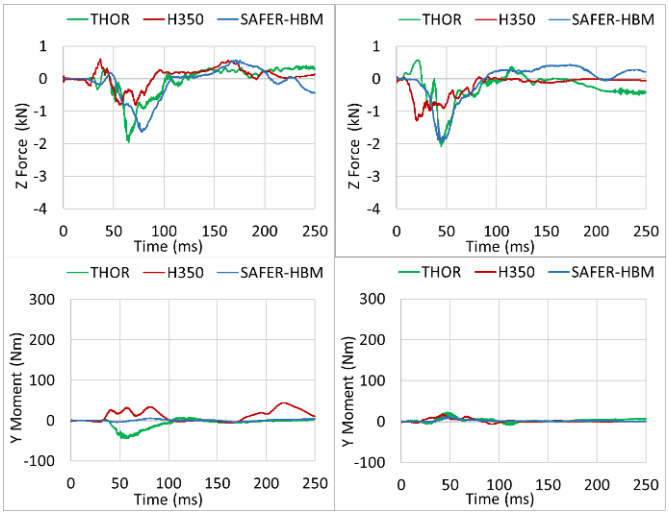

Fig. 13. Comparison of tension-compression force and flexion-extension moment in upper cervical spine among the occupant models for the simulated variations: rotating backrest (in the left), fixed backrest (in the right)

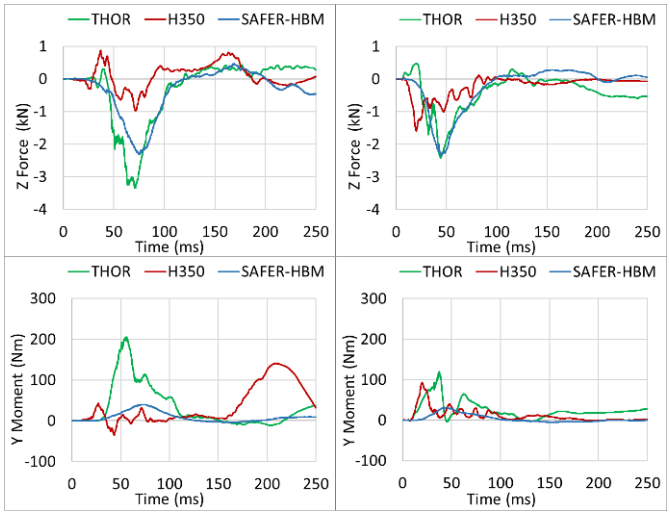

Fig. 14. Comparison of tension-compression force and flexion-extension moment in lower cervical spine among the occupant models for the simulated variations: rotating backrest (in the left), fixed backrest (in the right)

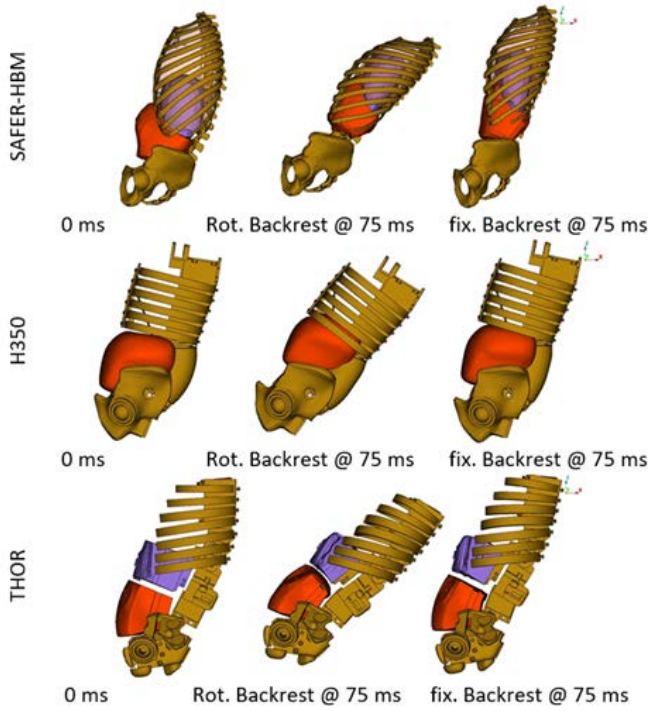

Fig. 15. Deformation and displacement in abdominal organs for the simulated variations

Figure 15 shows the inertially induced movement and deformation in the abdominal organs at the end of loading phase in all three occupant models. The upper and lower abdominal organs in the SAFER-HBM move substantially inside the thoracic cavity that the volume of lungs is compressed by more than 50%. In comparison to SAFER-HBM, no such large organ displacement and deformation is visible in both the dummy models. While

the H350 abdominal insert moves about 60 mm upwards with nearly no compression, the abdominal organs in THOR gets compressed by about 20-25 mm but remains tightly attached to the nearby hard structure.

IV. DISCUSSION

Initial position of the SAFER-HBM could be better matched to H350, whereas it could not be better matched for the THOR. As mentioned before, a gap remains between the THOR's back to seat backrest because of which the THOR moves initially freely until its back touches the seat backrest. This could possibly explain the THOR sliding comparatively higher compared to other occupant models. Due to this sliding, THOR upper body engages with the seat back relatively higher and thus farther from the pivot point of seat backrest, resulting in having larger moment arm. This explains the reason for inducing comparatively higher seat back rotation by THOR in the rotating back rest case and also for producing the higher contact force in the fixed back rest case. Differences in the contact force and seat back rotation between SAFER-HBM and H350 could be attributed to the differences in their upper body mass distribution and to some extent the inertial effects of the inner organs in the SAFER-HBM.

The peak displacements in the THOR seem to be relatively close to that in the SAFER-HBM, whereas they remain substantially smaller in H350 for all trajectories for both the backrest stiffness cases. One exception for the THOR is the peak chest displacement with the rotating backrest, which is smaller as compared to SAFER-HBM in both x and z directions by 45 mm and 20mm, respectively. One plausible reason could be that the T4 (chest) marker in the SAFER-HBM is about 90 mm above in z-direction compared to that in the THOR. This implies that for a given rotation in the backrest the higher marker position can produce more X and Z displacements. This could be verified with the fixed backrest case where there is no rotation in the backrest, thereby reducing the effects of marker initial positions on the trajectories. It is seen that the peak X and Z displacements in the THOR comes closer to that in the SAFER-HBM (only 10 mm difference in x-direction) with the fixed backrest. However, the same argument does not explain the lower peak chest displacements in the H350 in the rotating backrest compared to other occupant models. Because even with the fixed backrest case, the peak chest displacement in H350 remains lower by more than 35 mm in x-direction compared to others. Since the fixed backrest case offers no rotation in the backrest, the upper body kinematics seems to be governed by deformation in the spinal column in combination with pelvis rotation. This indicates that the lower displacements in the H350 could be attributed to limitation in its spinal column design which is comprised of a deformable lumbar block connected to a rigid thoracic spine block. Thus, the entire upper body in the H350 moves only with the deformation in the lumbar spine. In comparison, there are several joints in the THOR spine which allows relative rotations in the lumbar and the thoracic spine and thus helps the THOR in predicting trajectories closer to that in SAFER-HBM.

Other differences could be noticed in the pelvis trajectories. In the rotating backrest, the THOR pelvis trajectory closely follows the SAFER-HBM with the peak differences of only 5 mm and 15 mm in x and z directions. Whereas, the pelvis in the H350 initially follows the similar trajectory to that in SAFER-HBM however travels almost 55 mm less in x-direction and 22 mm in z-direction as compared to SAFER-HBM. The closer response of THOR over H350 could be attributed to its pelvic structure and flesh which are substantially different from those of the H350. While, THOR's flesh is segmented to allow full range of motion at the hip joint with having less coupling to femur motion, the H350's extension of pelvic flesh to the proximal thigh reduces the femur range of motion and thereby increases the overall stiffness of the hip joint. In the fixed backrest, the pelvis in the THOR continues to lift in positive z-direction whereas, both SAFER-HBM and H350 go in the negative z-direction. It is observed for both SAFER-HBM and H350 that the lower legs are restricted by the front of the seat-pan which pulls the occupant towards the seat-pan. Whereas this interaction is missing with the THOR, possibly because the upper leg lifts the lower leg in such a way that it does not hit the seat-pan.

Furthermore, while comparing the chest and pelvis accelerations, both H350 and THOR predict peak accelerations close to that in SAFER-HBM, however, THOR performs marginally closer to SAFER-HBM than the H350. This indicates that both the dummy models have overall similar kinematics responses.

One of the major differences between THOR and H350 is seen in their chest deflections. Both THOR and SAFER-HBM predict higher chest deflections (above 35 mm) and remains with in close range (difference of 10 mm), whereas, H350 predicts very low value (peak value of only 5 mm). Comparing the absolute value of chest deflection among them here is just not an indication of their ability to predict thoracic injury because there are

no thoracic injury risk functions for rear impacts. However, comparing physical deformation behavior shows that deformation in THOR chest (shown in Figure 10 (b)) with rotation in lower ribs follow as in SAFER-HBM with underlying design limitations. The joints in thoracic spine in the THOR allows relative rotation and thereby allows ribs to rotate whereas geometry and structure of ribs allow deformation. In contrast, such deformation pattern is largely missing in H350. It is interesting to note here that in the absence of any diagonal belt interacting with the dummy during the loading phase for rearward-facing seat configuration, the chest deflection is primarily induced by inertia due to applied crash pulse. Since, the chest accelerations in both THOR and H350 are almost same (as shown in Figure 8), the H350 is not able to transform the acceleration into chest deformation whereas the THOR could do so. The inability of H350 could be linked to its rigid thoracic spine in combination with ribs geometry and structural design. The THOR is benefitted here as well because it has better approximated human rib geometry and structure along with the joints in thoracic spine.

Comparing the lumbar spine response, both THOR and H350 overpredict the force and moment as compared to SAFER-HBM with a high margin both in tension-compression force (Z-force) and flexion-extension moment (Y-moment). However, despite differences in the lumbar spine designs between THOR and H350, they seem to behave similar in rear facing impact with minor differences in their compressive and bending stiffnesses. Moreover, the differences in their stiffnesses further reduce in the fixed backrest case.

Another finding is the differences in neck loading. While observing deformation in the neck, both SAFER-HBM and THOR exhibit high deformations whereas neck in H350 remains almost intact. This indicates that for the given deformation, neck in the H350 seems stiffest as compared to other occupant models.

A large displacement is predicted by the SAFER-HBM in abdominal organs. If this is to be believed, such a large displacement can cause high compression leading to organ injuries. In addition, this could also lead to increase in pressure inside the thoracic cavity, which could affect the chest deformation and eventually affect the risk of rib fractures. In comparison to SAFER-HBM, both the dummy models could not capture this aspect of deformation. Therefore, it would not be possible with both H350 and THOR to quantify how inertially induced dynamic loading resulting from organ displacement could affect the chest deflection.

Unlike with conventional forward-facing seat configuration where the deformations in occupant are induced while interacting with the restraint systems: belts and airbag; the inertially induced deformations may become more important source of injuries in the rearward-facing seat configuration. This needs to be investigated with PMHS tests in future. If this effect were to be confirmed in PMHS tests, ATDs would need to be modified to represent inertial loading in a biofidelic manner.

Validation of the occupant models for rear facing high speed impact is the main limitation of the current study. Although it could be argued that the SAFER-HBM should exhibit a more biofidelic response compared to the ATDs, due to its detailed representation of the human anatomy, it is important to mention that none of the occupant models are validated for rear facing impact. Therefore, the results of this study should be understood only as a model comparison and not as a validation of the ATDs, since none of the models necessarily represent human response in a biofidelic manner.

V. CONCLUSIONS

The responses of the THOR, the H350 and the SAFER-HBM are compared among each other for the rearward-facing seat configuration in full-frontal impact according to FMVSS208 at 56 km/h. THOR was more similar to SAFER-HBM in several aspects, possibly due to its spine design with inclusion of flexible joints in thoracic-lumbar region, than H350. Both ATDs match kinematics and accelerations of the SAFER HBM reasonably well. Only THOR and SAFER HBM can capture inertially induced deformation in the chest.

VI. ACKNOWLEDGEMENT

Authors would like to thank to colleagues Nils Lübbe and Martin Ostling from Autoliv research for providing valuable feedbacks which helped in improving the content of the paper.

VII. REFERENCES

[1] Jorlöv, S., Bohman, K., Larsson, A. (2017) Seating positions and activities in highly automated cars – a qualitative study of future automated driving scenarios. *Proc. IRCOBI Conference*, 2017, Belgium

[2] “Preparing for the Future of Transportation Automated Vehicles 3.0”.Internet:[https://www.transportation.gov/av/3/preparing-future-transportation-automated-vehicles-3], [15-03-2020]
[3] Lubbe, N., Jeppsson, H., Ranjbar, A., Fredriksson, J., Bärgman, J., Östling, M. (2018) Predicted road traffic fatalities in Germany: the potential and limitations of vehicle safety technologies from passive safety to highly automated driving. *Proc. IRCOBI Conference*, 2018, Athens (Greece)
[4] Östling, M., Lubbe, N., Jeppsson, H., Puthan, P. (2019) Passenger car safety beyond ADAS: defining remaining accident configurations as future priorities. Paper Number 19-0091, *Proc. 26th ESV Conference*, 2019, Eindhoven, Netherlands
[5] Östling, M., Lubbe, N., Jeppsson, H. (2019) Predicted crash configurations for autonomous driving vehicles in mixed German traffic for the evaluation of occupant restraint system. *VDI conference*, 2019, Hannover
[6] Zellmer, H., Lubbe, N., Sander, U. (2018) Assessing the injury risk of car occupants on rearward facing seats – an analysis of GIDAS cases. *8th ESAR Conference*, 2018, Hannover, Germany
[7] Edwards, M. A.; Brumbelow, M. L.; Trempel, R. E.; Gorjanc, T. C. (2019) Seat design characteristics affecting occupant safety in low and high-severity rear-impact collisions*, Proc. IRCOBI Conference,* 2019, Florence
[8] Sengottu, V. S., Andreas, H. (2018) Development of occupant restraint systems for future seating positions in fully or semi autonomous vehicles. *Proc. SAEINDIA,* 2018
[9] “Biomechanical Responses and Injuries of PMHS in Rear Facing Alternative Seating Configurations” Internet:[https://www.nhtsa.gov/sites/nhtsa.dot.gov/files/documents/biomechanical_responses_and_injuries_of_pmhs_in_rear_facing_alternative_seating_configurations_tag.pdf], [15-03-2020]
[10] Tatem, W., Gabler, G. (2017) Preliminary analysis of serious-to-fatal injury in rear impact crashes in the United States*, Proc. IRCOBI Conference*, 2017, Antwerp, Belgium
[11] James W. Saunders III, Louis N. Molino, Shashi Kuppa, Felicia L. McKoy. (2003) Performance of seating systems in a FMVSS no. 301 rear impact crash test. *Proc. 18th ESV-Conference,* 2003, Nagoya, Japan
[12] David C. Viano, Chantal S. Parenteau, Roger Burnett, Priya Prasad. (2017) Occupant responses in conventional and ABTS seats in high-speed rear sled tests. *Traffic Injury Prevention* 2017
[13] Kitagawa, Y., Hayashi, S., Yamada, K., Gotoh, M. (2017) Occupant kinematics in simulated autonomous driving vehicle collisions: influence of seating position, direction and angle. *Stapp Car Crash Journal*, Vol. 61, 2017
[14] Jin, X., Hou, H., Shen, M., Wu, H., Yang, K. Y. (2018) Occupant kinematics and biomechanics with rotatable seat in autonomous vehicle collision: a preliminary concept and strategy. *Proc. IRCOBI Conference*, 2018, Athens, Greece
[15] Katagiri, M.; Zhao, J.; Lee, S.; Moorhouse, K.; Kang, Y-S. (2019) Biofidelity evaluation of ghbmc male occupant models in rear impacts. *Proceedings IRCOBI Conference,* 2019, Florence (Italy)
[16] Zellmer, H.; Manneck, F. (2019) Assessing injury risk of car occupants on rearward facing seats in a full-frontal impact – sled tests in a generic test environment. *Proc. 26th ESV Conference*, 2019, Eindhoven,
[17] Zellmer, H.; Soni, A., Schilling, S., Eickhoff, B. Injury risk on rearward facing seats in frontal impact – sled tests and simulation is a generic test environment, *VDI Conference*, 2019
[18] User Manual Safer – HBM v9

Appendix -A1: SUMMARY OF VALIDATION RESULTS

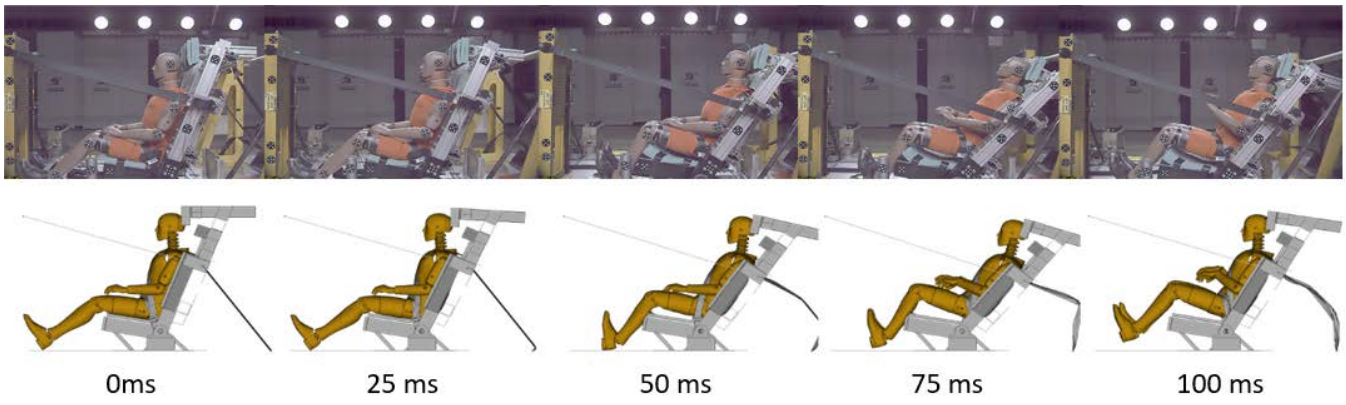

Fig. A1. Comparison of H350 kinematics in testing (above) and simulation (below) at different instances

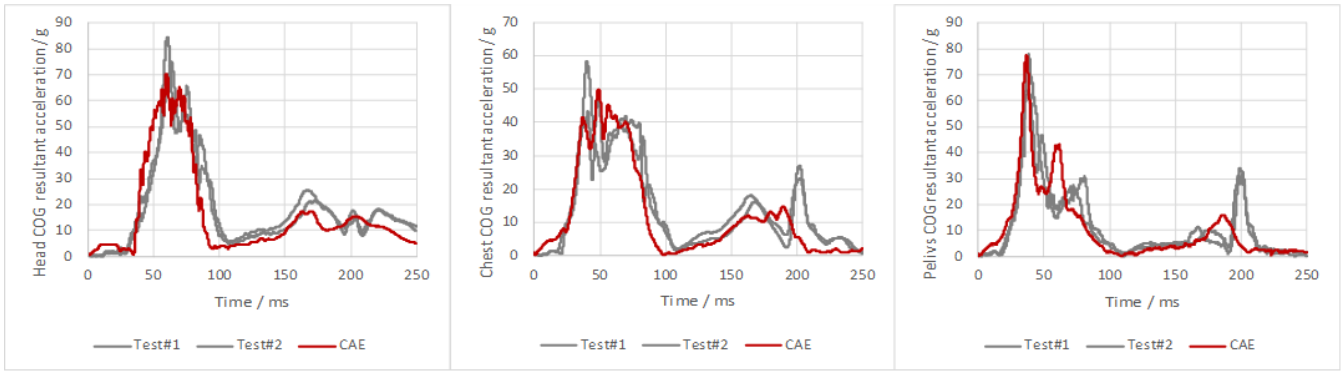

Fig. A2. Comparison between simulation and testing for Head (in the left), Chest (in the middle) and Pelvis (in the right) accelerations

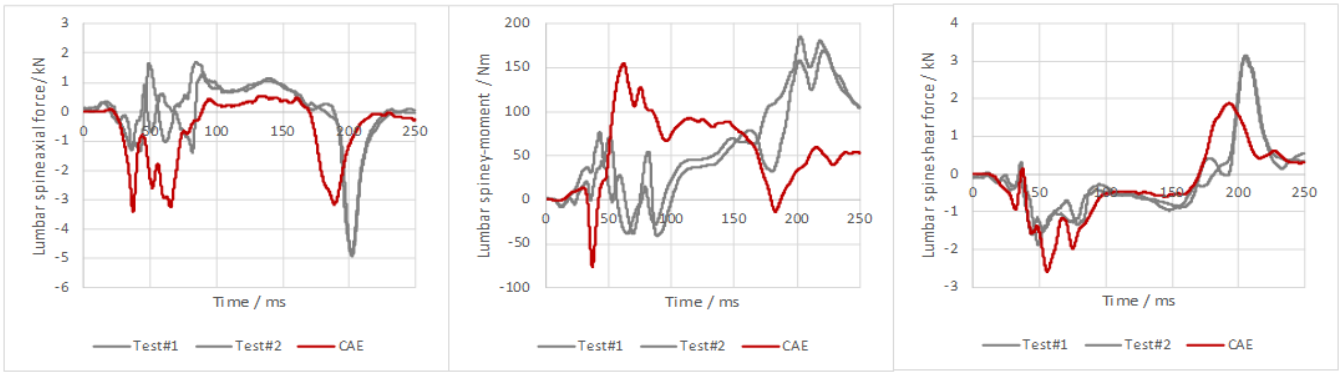

Fig. A3. Comparison between simulation and testing for lumbar spine axial force (in the left), Y-moment (in the middle) and shear force (in the right)

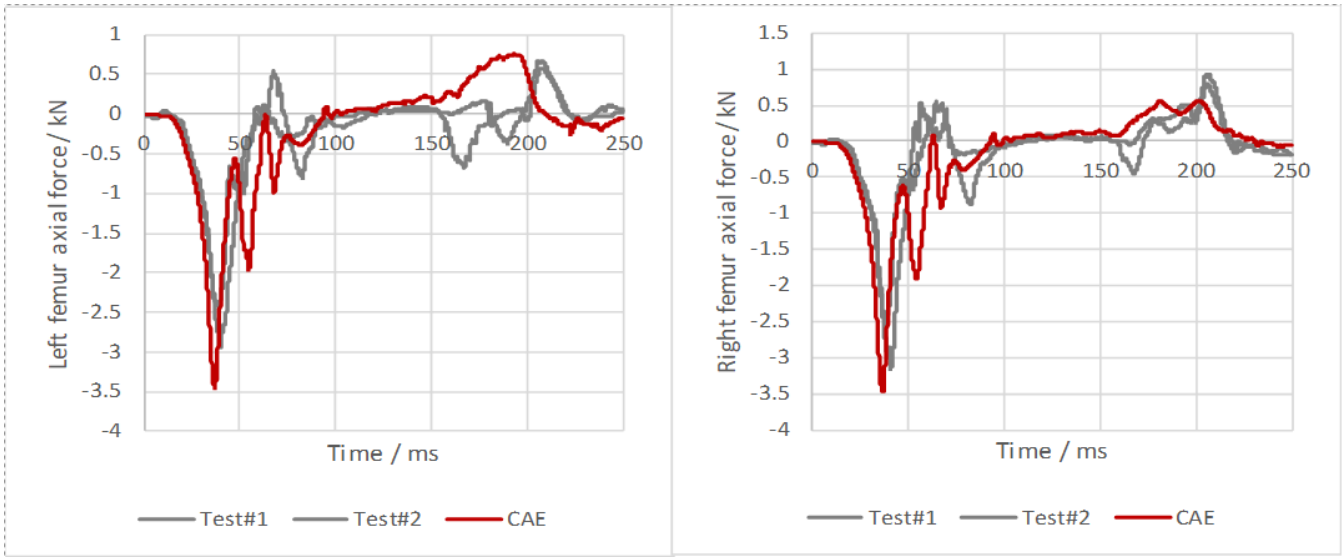

Fig. A4. Comparison between simulation and testing for left femur (in the left) and right femur (in the right) axial force

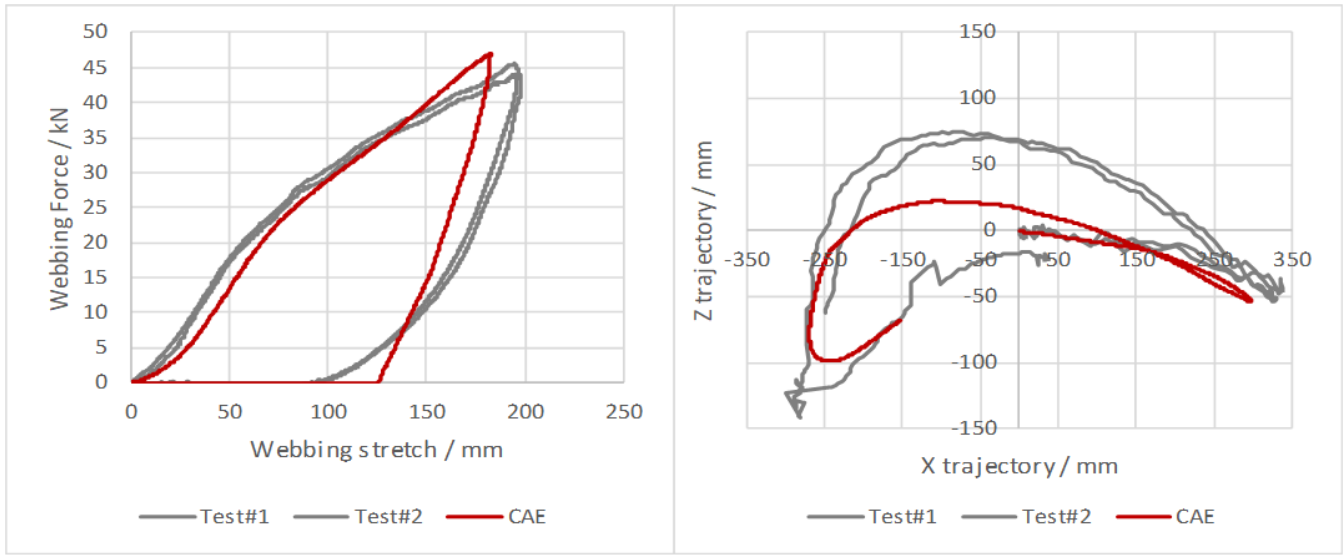

Fig. A5. Comparison between simulation and testing for front webbing force to webbing stretch (in the left) and head trajectory (in the right)

Appendix -B1: CHEST DEFLECTION MEASUREMENT IN SAFER-HBM

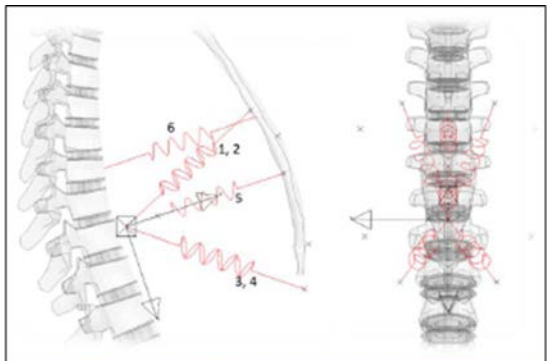

Nr	Discrete ID	Name
5	44200105	Chest_def_sternum_center_rib_6
6	44203001	Chest_def_ssternum_center_rib_3

Fig. B1. 6 Discrete elements have been implemented for easy chest deflection measurement in SAFER-HBM